Novel Formulation of Adaptive MPC as EKF Using ANN Model: Multiproduct Semibatch Polymerization Reactor Case Study

Reddi Kamesh and Kalipatnapu Yamuna Rani

***Abstract*— In this paper, a novel formulation for nonlinear model predictive control (MPC) has been proposed incorporating the extended Kalman filter (EKF) control concept using a purely data-driven artificial neural network (ANN) model based on measurements for supervisory control. The proposed scheme consists of two modules focusing on online parameter estimation based on past measurements and control estimation over control horizon based on minimizing the deviation of model output predictions from set points along the prediction horizon. An industrial case study for temperature control of a multiproduct semibatch polymerization reactor posed as a challenge problem has been considered as a test bed to apply the proposed ANN-EKFMPC strategy at supervisory level as a cascade control configuration along with proportional integral controller [ANN-EKFMPC with PI (ANN-EKFMPC-PI)]. The proposed approach is formulated incorporating all aspects of MPC including move suppression factor for control effort minimization and constraint-handling capability including terminal constraints. The nominal stability analysis and offset-free tracking capabilities of the proposed controller are proved. Its performance is evaluated by comparison with a standard MPC-based cascade control approach using the same adaptive ANN model. The ANN-EKFMPC-PI control configuration has shown better controller performance in terms of temperature tracking, smoother input profiles, as well as constraint-handling ability compared with the ANN-MPC with PI approach for two products in summer and winter. The proposed scheme is found to be versatile although it is based on a purely data-driven model with online parameter estimation.**

***Index Terms*— Artificial neural network extended Kalman filter model predictive control with proportional integral (ANN-EKFMPC-PI) cascade control, ANN-MPC with PI (ANN-MPC-PI) cascade control, EKF-based online parameter estimation, MPC formulation as EKF, multiproduct semibatch polymerization reactor, temperature tracking.**

I. INTRODUCTION

MODEL predictive control (MPC) has been one of the most widely accepted control techniques both academically and industrially, and its nonlinear version has attracted more attention recently. Reviews regarding MPC techniques can be seen in [1]–[3]. Mahindrakar and Hahn [4] evaluated the performance of different MPC strategies for reactive distillation column control for disturbance rejection compared with decentralized PI control. Ghaffari *et al.* [5] proposed a robust MPC control law for additive uncertain nonlinear systems, and the effectiveness of their approach is illustrated for industrial continuous stirred tank reactor control problems with two and three states.

Peterson *et al*. [6] have applied nonlinear dynamic matrix control for semibatch reactors through simulations, and Karaduman *et al*. [7] have implemented MPC for real-time temperature control in a polymerization reactor problem. Nonlinear MPC (NMPC) has been used by many researchers in different applications: shrinking horizon NMPC strategy for batch crystallization control [8] and fed-batch fermenter control problem [9]. Recently, Lucia *et al.* [10] applied multistage NMPC to a semibatch polymerization reactor under uncertainty.

The most difficult and time-consuming step in the implementation of NMPC is the development of a reliable first principles model for the process under consideration. In addition, most of these schemes are developed under the assumption that all the state variables are either measured or can be accurately estimated from the available measurements, which may not be a realistic assumption in many practical situations. Data-driven black-box models, on the other hand, have gained significance as alternatives to first principles models.

During the last decade, artificial neural networks (ANNs) have gained importance as versatile data driven structures for modeling nonlinear steady state as well as dynamic processes. Rani and Patwardhan [11] have proposed a novel data-driven approach for modeling and optimal set point generation for a batch/semibatch process with the help of ANNs. There have also been some attempts to use ANNs for trajectory tracking in batch reactors. Chen and Huang [12] have employed ANNs to model a batch reactor and used its linearized version at every sampling instant to update the tuning parameters of a PID controller. Xiong and Zhang [13] proposed a batch-to-batch iterative optimal control strategy based on recurrent neural network models and applied it to a methyl methacrylate polymerization reactor. Recently, Kumar and Almad [14] have developed a hybrid model containing a mechanistic model and a feed-forward neural network model with an MPC controller, to control the molecular weight of a batch bio-polymerization reactor.

Manuscript received February 22, 2016; revised June 15, 2016 and September 27, 2016; accepted September 29, 2016. Date of publication October 13, 2016; date of current version November 15, 2017. This work was supported by the CSIR XII Plan Project, INDUS MAGIC. *(Corresponding author: Kalipatnapu Yamuna Rani.)*

The authors are with the Chemical Engineering Division, Process Dynamics and Control Group, CSIR-Indian Institute of Chemical Technology, Hyderabad 500007, India, and also with the Academy of Scientific and Innovative, Hyderabad, India (e-mail: kyrani@iict.res.in).

This paper has supplementary downloadable material available at http://ieeexplore.ieee.org., provided by the author.

Color versions of one or more of the figures in this paper are available online at http://ieeexplore.ieee.org.

Digital Object Identifier 10.1109/TNNLS.2016.2614878

Extended Kalman filter (EKF) has been a well-known technique to estimate unmeasured states and unknown parameters from measured states to augment for limited state information in nonlinear-model-based control [15], [16]. Myers and Luecke [17] illustrated the applications of EKF for process control. Gao *et al.* [18] have proposed the estimation of control inputs using an EKF based on a neural network model. Application of their approach for level control resulted in offset, which was handled by the addition of a feedback compensating controller. An EKF-based recursive algorithm was proposed by Rivals and Personnaz [19] for training of feed-forward neural networks. They have shown that the estimation of weights by EKF is more efficient than by recursive and nonrecursive first-order training algorithms, and at least as good as the most efficient nonrecursive second-order algorithms. Rani and Swetha [20] have proposed the use of EKF controller along with EKF-based state and parameter estimation and have illustrated its applicability for batch reactor temperature control. Saengchan *et al.* [21] implemented MPC integrated with EKF to control the temperature of a batch crystallizer.

An industrial case study for a multiproduct semibatch polymerization reactor temperature control has been proposed in [22] as a challenge problem. Two approaches have been employed to control this problem, namely, direct control and cascade control approaches. In the former approach, temperature is the controlled variable and valve opening is the manipulated variable, whereas in the latter approach, the reactor temperature is controlled by the jacket temperature in the master loop and jacket temperature is controlled using valve opening as the manipulated input in the slave loop. With the help of the first approach, Rani [23] proposed a novel sensitivity compensating control approach combined with an extended external reset feedback method to handle sensitivity and input saturation with the application of Generic Model Control (GMC) based on an exact model. Different cascade control combinations with GMC and PI have been explored by Kamesh *et al.* [24] for this system based on the first principles model. Using the cascade control structure with simplified-model-based controllers together with estimation techniques, Clarke-Pringle and MacGregor [25] have proposed a nonlinear adaptive temperature control strategy, where some of the unknown process parameters are estimated using an EKF to find the jacket temperature set point for the slave controller in a cascade structure. Graichen *et al.* [26] have applied feed-forward control with online parameter estimation using EKF based on a calorimetric reactor model and a nonlinear model of the cooling system. Unscented Kalman filter has been employed to estimate the heat of reaction and heat transfer coefficient in the energy balance equation by Vasanthi *et al.* [27] in a self-tuning master control loop to maintain the reactor temperature in this problem within a tolerance limit of ± 0.6 K. Helbig *et al.* [28] have proposed a direct control strategy based on a simplified model-based MPC in combination with an EKF for controlling the temperature of the Chylla–Haase problem.

Ng and Hussain [29] have proposed the use of hybrid neural networks for the Chylla–Haase problem, where two networks are employed to estimate the unknown parameters in combination with the first principles mass and energy balance equations and a third network is used in a direct inverse control strategy to track the temperature set point and determine the jacket temperature set point. Rani [30] proposed novel sensitivity compensating control approach based on a purely data driven model, i.e., an autoregressive exogenous model with the application of GMC, whereas Rani and Patwardhan [31] have applied an offline trained neural network based GMC for direct temperature control of this system. Recently, a time-varying NN model has been developed for this system based on offline training, which has not yet been employed for any control studies [32].

In this paper, a purely data-driven adaptive-ANN-model-based MPC is proposed as a novel EKF formulation in cascaded form. In the EKFMPC formulation, the manipulated input values, which minimize the deviations of the set points from their predicted output values over the prediction horizon, are estimated over a control horizon. The first set of inputs is then implemented on the process before moving to the next time step. Further, unlike most of ANN-based control approaches, the ANN model in this paper is not an offline trained network. EKF is used to formulate parameter estimation problem to estimate the unknown parameters and is solved at every sampling instant to compensate for process/model mismatch. The earlier approach of Gao *et al.* [18] for single-step control estimation required the augmentation of a feedback control correction for offset-free performance. In this paper, the parameters of the ANN model (weights) are updated using an EKF for parameter estimation at every sampling instant and the updated ANN model is then employed for predictive control estimation. The semibatch polymerization reactor challenge control problem of Chylla and Haase [22] is considered to evaluate the applicability of the proposed approach.

II. Extended-Kalman-Filter-Based Model Predictive Control

An EKF computes the optimal state and/or parameter estimates of a nonlinear system at each sampling time using a linearized model and linear estimation principles. The estimation is on the basis of the assumption that a model describing the system is available and that the mean and covariances of measurement errors, inputs, and outputs are known. EKF is a well-known mathematical technique with extensive applications in state and parameter estimation.

Rani and Swetha [20] have proposed the use of EKF as a controller in addition to its use for state and parameter estimation. In the EKF formulated as a controller, the outputs are treated as states, whereas the control action is treated as a parameter. Further, the correction for EKF state estimation is based on minimizing the past measurement error for all the states and parameters, whereas in the EKF controller, the correction is based on minimizing the one-step-ahead predicted output deviation from its set point and is restricted to control action only, with states left uncorrected.

MPC is an optimization-based multivariable control strategy that uses a mathematical model, incorporated into a control algorithm to compute the control action to be implemented on the process. The approach is based on minimizing the deviation between the model predictions and set points over a prediction horizon to compute the control action over another smaller control horizon. This approach requires solving of an optimization problem at each sampling instant to find the control actions. EKF is well established as a versatile estimation technique, and therefore, in this paper, instead of solving an optimization problem, an iterative approach is proposed based on the extension of EKF controller concept to predictive control as an MPC formulation using a simple ANN model. The weights of the network are treated as the parameters for the ANN model to be estimated.

The proposed approach consists of two modules, namely, EKF-based parameter estimation for estimation of ANN weights and EKF-based predictive control computation using the updated ANN model. In the first module of this approach, the parameters are defined as the ANN weights, whereas the output prediction using the ANN model is the measurement equation with measurement noise of zero mean and known covariance. At every sampling instant, the parameters are updated on the basis of minimization of the deviation between the available measurement and its predicted value based on the past information.

The process model is represented as

$$\begin{aligned}\boldsymbol{\theta}_k &= \boldsymbol{\theta}_{k-1} + \boldsymbol{w}_{k-1}\\ y_k &= NN(y_{k-1}, \boldsymbol{\theta}_{k-1}, u_{k-1}) + \upsilon_k \end{aligned}\tag{1}$$

where u is the manipulated input, $\boldsymbol{\theta}$ is the parameter vector of dimension p, k denotes the present time, and$y_k$represents the output variable. The parameter uncertainty vector $\boldsymbol{w}$ and the measurement error υ are assumed to be white Gaussian random processes with zero mean and covariances $\boldsymbol{Q}$ and R, respectively.

The iterative-EKF-based parameter estimation equations for the above model are summarized as follows [19], [20].

1) *Parameter Propagation:*

$$\begin{aligned}\boldsymbol{\theta}_k^- &= \boldsymbol{\theta}_{k-1}^+ \quad \text{for first iteration, and}\\ \boldsymbol{\theta}_k^- &= \boldsymbol{\theta}_k^+ \quad \text{from second iteration.}\end{aligned}\tag{2}$$

2) *Covariance Propagation:*

$$\begin{aligned}\mathbf{P}_k^- &= \left(\mathbf{P}_{k-1}^+ + \mathbf{Q}\right) \quad \text{for first iteration, and}\\ \mathbf{P}_k^- &= \left(\mathbf{P}_k^+ + \mathbf{Q}\right) \quad \text{from second iteration.}\end{aligned}\tag{3}$$

3) *Kalman Gain:*

$$\mathbf{K}_k = \mathbf{P}_k^- \mathbf{G}_k^T \left[\mathbf{G}_k \mathbf{P}_k^- \mathbf{G}_k^T + R\right]^{-1}\tag{4}$$

where

$$\mathbf{G}_k = [\partial(NN)/\partial\boldsymbol{\theta}]_{\boldsymbol{\theta}_{k-1}^+}.\tag{5}$$

4) *Parameter Update:*

$$\boldsymbol{\theta}_k^+ = \boldsymbol{\theta}_k^- + \mathbf{K}_k\left[y_k^m - NN\left(y_{k-1}, \boldsymbol{\theta}_k^-, u_{k-1}\right)\right]\tag{6}$$

where y_k^m is the measured output at the kth sampling instant.

5) *Covariance Update:*

$$\mathbf{P}_k^+ = [\mathbf{I}_p - \mathbf{K}_k\mathbf{G}_k]\mathbf{P}_k^-\tag{7}$$

where $\boldsymbol{I}_p$ denotes the identity matrix of dimension $p \times p$. In the above equations, the superscript "–" indicates the values before measurement update, whereas the superscript "+" indicates the values after measurement update; $\boldsymbol{K}$ is the Kalman gain; and $\boldsymbol{P}$ is the initial parameter covariance, the process noise covariance is $\boldsymbol{Q}$, and the measurement error covariance is $\boldsymbol{R}$. These matrices are assumed to be constant diagonal matrices ($\boldsymbol{P} = \text{p0 } I$, $\boldsymbol{Q} = qI$, $\boldsymbol{R} = rI$), and the three parameters p0, q, and r are tuned to achieve the desired performance and $\boldsymbol{I}$ is the identity matrix.

The second module, proposed in this paper as EKFMPC, is derived on similar lines as an EKF parameter estimation algorithm, with the parameters replaced by control inputs over the control horizon. Further, the repeated use of the measurement equation is considered for predictions from the current sampling instant to the end of the prediction horizon and past measurements in EKF parameter estimation are replaced by future set points over the prediction horizon for EKFMPC formulation. The objective function is redefined to incorporate the MPC strategy and the control law is derived. As per the standard MPC practice, only the first of the computed control actions is implemented and the procedure is repeated at the next sampling instant. The prediction horizon is considered to be N, whereas the control horizon (Nc) is taken as unity. This assumption can be relaxed at the expense of additional computational effort and a slightly complicated problem formulation.

The ANN-model-based EKFMPC formulation considering control horizon as unity in the second module is derived as follows.

The process is represented as

$$\begin{aligned}u_k &= u_{k-1} + wc_{k-1}\\ \mathbf{y}_k^d &= \mathbf{h}\left(u_k, \boldsymbol{\theta}_k^+, \mathbf{y}_{k-1}^d\right) + \mathbf{vc}_k\end{aligned}\tag{8}$$

where

$$\begin{aligned}\mathbf{h}\left(u_k, \boldsymbol{\theta}_k^+, \mathbf{y}_{k-1}^d\right) &= \left\{\tilde{\hat{y}}_{k+i};\ i = 1, \ldots, N\right\}\\ &\quad \text{if } i = 1,\ \hat{y}_{k+1} = NN\left(y_k^m, \boldsymbol{\theta}_k^+, u_k^-\right)\\ \tilde{\hat{y}}_{k+1} &= \hat{y}_{k+1} + e_k\\ &\quad \text{for } i > 1,\ \hat{y}_{k+i} = NN\left(\hat{y}_{k+i-1}, \boldsymbol{\theta}_k^+, u_k^-\right)\\ \tilde{\hat{y}}_{k+i} &= \hat{y}_{k+i} + e_k\\ &\quad \text{where } e_k = \left[y_k^m - NN(y_{k-1}, \boldsymbol{\theta}_k^+, u_{k-1})\right]\end{aligned}\tag{9}$$

where $\mathbf{y}_k^d$ represents the predicted output variable vector of dimension N, $\mathbf{h}$ is a vector function, and e_k represents the feedback correction term for the process model mismatch from the latest measurement, as per the MPC practice. The input uncertainty wc and the set point deviation error vector $\mathbf{vc}$ are assumed to be white Gaussian random processes with zero mean and covariances Qc and $\mathbf{Rc}$, respectively. The assumption for the input model in this paper is similar to the assumption for parameters like heat release in batch reactions for EKF-based state and parameter estimation [33]. The parameters updated in the first module are used as such in the propagation and correction steps as follows.

1) *Control Propagation:*

$$\begin{aligned} u_k^- &= u_{k-1}^+ \quad \text{for first iteration and} \\ u_k^- &= u_k^+ \quad \text{from the second iteration} \\ \mathbf{y}_k^d &= \mathbf{h}\big(u_k^-, \boldsymbol{\theta}_k^+, \mathbf{y}_{k-1}^d\big). \end{aligned} \tag{10}$$

2) *Covariance Propagation:* Covariance is defined as

$$Pc_k^- = E\big[\big(u_k - u_k^-\big)\big(u_k - u_k^-\big)^T\big]. \tag{11}$$

This equation can be transformed into

$$\begin{aligned} &\text{For the first iteration} \\ &\quad Pc_k^- = Pc_{k-1}^+ + Qc \\ &\text{From the second iteration} \\ &\quad Pc_k^- = Pc_k^+ + Qc \end{aligned} \tag{12}$$

where Pc is control input covariance with a dimension of control horizon and Qc is the controller noise covariance.

In accordance with the EKF derivation method, the corrected control action is assumed to be linearly dependent on the output prediction. Further, assuming that there is no bias between the control action to be implemented (u_k) and the computed corrected control action (u_k^+), the correction step (or the *control update* step) is given as

$$u_k^+ = u_k^- + \mathbf{Kc}_k\big(\mathbf{y}_k^{\text{set}} - \mathbf{h}\big(u_k^-, \boldsymbol{\theta}_k^+, \mathbf{y}_{k-1}^d\big)\big) \tag{13}$$

where $\mathbf{y}_k^{\text{set}}$ is the vector of target values for the predicted outputs over the prediction horizon starting at the kth sampling instant. $\mathbf{Kc}_k$ is the control Kalman gain.

In order to derive MPC law, the objective function is defined as

$$\begin{aligned} \text{Obj} &\equiv \text{trace}\left\{\begin{array}{l} E\big[\big(u_k - u_k^+\big)\big(u_k - u_k^+\big)^T\big] \\ +E\big[\lambda\big(\big(u_k^+ - u_{k-1}^+\big)\big(u_k^+ - u_{k-1}^+\big)^T\big)\big] \end{array}\right\} \\ &= \text{trace}\left\{\begin{array}{l} \big(I - \mathbf{Kc}_k\mathbf{Gc}_k^T\big)Pc_k^-\big(I - \mathbf{Kc}_k\mathbf{Gc}_k\big)^T \\ +\mathbf{Kc}_k\mathbf{Rc}_k\mathbf{Kc}_k^T + \lambda\ \mathbf{Kc}_k \\ \times\big(\mathbf{Gc}_k\big(Pc_k^-\big)\mathbf{Gc}_k^T + \mathbf{Rc}_k\big)\mathbf{Kc}_k^T \end{array}\right\} \end{aligned} \tag{14}$$

where λ is the move suppression factor and

$$\mathbf{Gc}_k = [\partial\mathbf{h}/\partial u]_{\theta_k^+, u_k^-}. \tag{15}$$

The first term in the objective function is the updated covariance estimate. The second term in the objective function is added in this paper to minimize the control effort. The optimal value of Kalman gain is obtained by differentiating (14) with respect to $\mathbf{Kc}_k$ and equating it to zero. The resulting expressions for control Kalman gain and control covariance update are given as follows.

1) *Kalman Gain:*

$$\mathbf{Kc}_k = \frac{Pc_k^-\mathbf{Gc}_k^T}{(1+\lambda)}\big[\mathbf{Gc}_k Pc_k^- \mathbf{Gc}_k^T + \mathbf{Rc}_k\big]^{-1}. \tag{16}$$

2) *Covariance Update:*

$$Pc_k^+ = [\mathbf{I} - \mathbf{Kc}_k\mathbf{Gc}_k]Pc_k^- - \left(\frac{\lambda}{(1+\lambda)}\right)Pc_k^-\mathbf{Gc}_k^T\mathbf{Kc}_k^T. \tag{17}$$

The measurement covariance matrix $\mathbf{Rc_k}$ with a dimension of $(N \times N)$ is updated during the iterative control computation according to the equation reported by Gao *et al.* [18]

$$\mathbf{Rc}_k(i) = \mathbf{Rc}_k(i-1) + \frac{1}{i}\left[\begin{array}{l} \big(\mathbf{y}_k^{\text{set}} - \mathbf{h}\big(u_k^-, \boldsymbol{\theta}_k^+, \mathbf{y}_{k-1}^d\big)\big) \\ \cdot\big(\mathbf{y}_k^{\text{set}} - \mathbf{h}\big(u_k^-, \boldsymbol{\theta}_k^+, \mathbf{y}_{k-1}^d\big)\big)^T \\ -\mathbf{Rc}_k(i-1) \end{array}\right] \tag{18}$$

where i is the iteration number.

The above development has not considered handling of constraints. The input constraints can be handled directly as hard bounds imposed on the computed control actions. To handle the output constraints, the derivation is continued from the updated estimates of control and covariance. The output constraints are expressed as

$$\mathbf{y}_c \leq \mathbf{y}^{\text{lim}} \tag{19}$$

where

$$\mathbf{y}_c = [\tilde{\hat{y}}_{k+1}; -\tilde{\hat{y}}_{k+1}] \quad \text{and}\ \mathbf{y}^{\text{lim}} = [y^{\max}; y^{\min}]. \tag{20}$$

In this formulation, constraints are imposed only on the first step of prediction rather than on the entire prediction horizon since the implementation is carried out only for a single step. At a given sampling instant, only one of these constraints or none of these constraints is violated. It is not straightforward to formulate inequality constraints without solving an optimization problem. This problem is handled by checking for the above constraint violations, and only in the presence of constraint violation, the formulation is attempted as an equality-constrained formulation. To derive the constrained control law, the objective function is defined as

$$\text{Objc} = \text{trace}\big(E\big[\big(u_k - u_k^{++}\big)\big(u_k - u_k^{++}\big)^T\big]\big) = \text{tr}\big(P_k^{++}\big) \tag{21}$$

where u_k^{++} is used to denote the control estimate corrected with respect to satisfaction of constraints. The corrected control action compensated for constraint handling can be represented by the following equation:

$$u_k^{++} = u_k^+ + Kc_k^{\text{con}}(\mathbf{y}^{\text{lim}} - \mathbf{y}_c) \tag{22}$$

$$\begin{aligned} Pc_k^{++} &= Pc_k^+ - Kc_k^{\text{con}}Gc_k^{\text{con}}Pc_k^+ - Pc_k^+\left(Gc_k^{\text{con}}\right)^T\left(Kc_k^{\text{con}}\right)^T \\ &\quad + Kc_k^{\text{con}}Gc_k^{\text{con}}Pc_k^+\left(G_{c_k}^{\text{con}}\right)^T\left(Kc_k^{\text{con}}\right)^T \end{aligned} \tag{23}$$

where

$$Gc_k^{\text{con}} = \left[\frac{\partial y_c}{\partial u}\right]_{u_k^+}. \tag{24}$$

On substitution of the appropriate expressions into the objective function and linearization of the constraints expression, and equating the derivative of the objective function with respect to Kc_k^{con} to zero, we obtain the following.

Constrained Kalman Gain:

$$Kc_k^{\text{con}} = Pc_k^+\big(Gc_k^{\text{con}}\big)^T\big[Gc_k^{\text{con}}Pc_k^+\big(Gc_k^{\text{con}}\big)^T\big]^{-1}. \tag{25}$$

The corrected covariance is then obtained as

$$Pc_k^{++} = \left(I - Kc_k^{\text{con}} Gc_k^{\text{con}}\right) Pc_k^{+}. \tag{26}$$

Further, in order to ascertain the stability of the proposed control approach, a terminal constraint is also imposed in this strategy. This is defined as

$$\tilde{\hat{\mathbf{y}}}_{k+N+1|k} = \mathbf{y}^{\text{set}}. \tag{27}$$

This equality constraint is converted into two inequality constraints with a small margin ε as

$$\mathbf{y}_c \leq \mathbf{y}_{\text{lim}}^{\text{set}} \tag{28}$$

where

$$\mathbf{y}_c = \left[\tilde{\hat{y}}_{k+N+1}; -\tilde{\hat{y}}_{k+N+1}\right] \quad \text{and } \mathbf{y}_{\text{lim}}^{\text{set}} = \left[y^{\text{set}} + \varepsilon; -y^{\text{set}} + \varepsilon\right]. \tag{29}$$

To derive the terminal constraint control law, the objective function is defined similar to (21) and the corrected control action compensated for terminal constraint handling can be represented by the following equation:

$$u_k^{+++} = u_k^{++} + Kc_k^{\text{ter}}\left(\mathbf{y}_{\text{lim}}^{\text{set}} - \mathbf{y}_c\right). \tag{30}$$

Similar to (23)–(26), the following equations are derived for terminal constraint covariance update and Kalman gain calculations:

$$\begin{aligned} &Pc_k^{+++} \\ &= Pc_k^{++} - Kc_k^{\text{ter}} Gc_k^{\text{ter}} Pc_k^{++} - Pc_k^{++}\left(Gc_k^{\text{ter}}\right)^T \left(Kc_k^{\text{ter}}\right)^T \\ &\quad + Kc_k^{\text{ter}} Gc_k^{\text{ter}} Pc_k^{++}\left(G_{c_k}^{\text{ter}}\right)^T \left(Kc_k^{\text{ter}}\right)^T \end{aligned} \tag{31}$$

where

$$Gc_k^{\text{ter}} = \left[\frac{\partial y_c}{\partial u}\right]_{u_k^{++}}. \tag{32}$$

1) *Constrained Kalman Gain:*

$$Kc_k^{\text{ter}} = Pc_k^{++}\left(Gc_k^{\text{ter}}\right)^T \left[Gc_k^{\text{ter}} Pc_k^{++}\left(Gc_k^{\text{ter}}\right)^T\right]^{-1}. \tag{33}$$

2) *Corrected Covariance:*

$$Pc_k^{+++} = \left(I - Kc_k^{\text{ter}} Gc_k^{\text{ter}}\right) Pc_k^{++}. \tag{34}$$

The above equations can be optionally used depending on the existence of constraints and terminal constraints violations in the predicted outputs. In the absence of constraints violations, the formulation of (10)–(18) is applicable. The final set of constrained EKF-based control calculations have a form similar to that reported by Ungarala *et al.* [34] for constrained EKF state estimation.

The above control approach can be applied at regulatory level to determine the manipulated control variable directly, or can be used as a master controller at the supervisory level to provide the set points for a slave controller for implementation. In this paper, this approach is applied for supervisory control to define the set points for a regulatory controller. The scheme is illustrated with the help of a block diagram shown in Fig. 1.

The algorithm for the proposed ANN-EKFMPC controller including both the modules is summarized as follows.

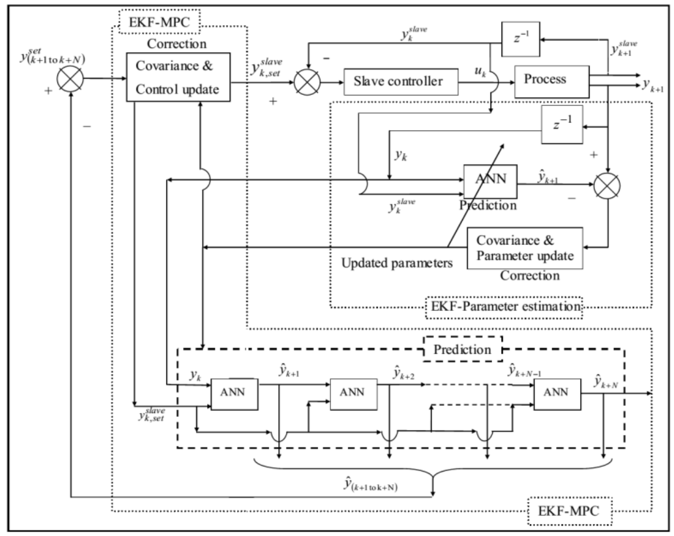

Fig. 1. Block diagram for adaptive ANN-EKFMPC supervisory controller.

1) Initialize the covariance matrices for parameter estimation ($\boldsymbol{P}_0$, $\boldsymbol{Q}$, and $\boldsymbol{R}$) as diagonal matrices (constants, i.e., p_0, q, and r times identity matrices).
2) Initialize the covariance matrices for control estimation ($\boldsymbol{Pc}_0$, $\boldsymbol{Qc}$, and $\boldsymbol{Rc}$) as diagonal matrices (constants, i.e., p_{c0}, q_c, and r_c times identity matrices).
3) With the help of the measurements of the output variables, perform EKF-based parameter estimation using (1)–(7).
4) Using the corrected values of the parameters from step 3, perform iterative EKF-based predictive control estimation by the following steps.
   a) Control propagation as per (10).
   b) Covariance propagation by (12).
   c) Control Kalman gain computation by (16).
   d) Control update by (13).
   e) Covariance update by (17).
   f) Check for constraint violations for the first prediction; if there are no constraint violations, go to step h. Otherwise, proceed to the next step.
   g) Compute the constraint correction Kalman gain for constrained control update by (22), the first prediction by (25), and constrained covariance update by (26). Replace updated covariance Pc_k^{+} with constrained covariance update Pc_k^{++} for use in covariance propagation (12) for the next iteration.
   h) Check for terminal constraint violations for the last prediction; if there are no constraints violations, go to step (j). Otherwise, proceed to the next step.
   i) Compute the terminal constraint correction Kalman gain by (33), terminal constraint control update by (30) and covariance update by (34). Replace the updated constrained covariance Pc_k^{+} with the terminal constrained covariance update Pc_k^{+++} for use in covariance propagation (12) for the next iteration.

j) Check for convergence. Convergence criteria employed for termination of the iterative procedure are as follows.
   i) Achieving the desired performance, i.e., the tracking error, defined as the average error between the set value and the output prediction, is less than a predefined threshold value (of the order of 10^{-3}).
   ii) The difference in control action computed in consecutive iterations is less than a prescribed small limit (of the order of 10^{-6}).
   iii) Reaching the input bounds.
   iv) Crossing the maximum number of iterations (given as a sufficiently large number, say 1000). This results in the set point values for the regulatory control loop.

5) Compute the regulatory control loop calculations using the set points determined in step 4.
6) Implement the control action on the process and shift to the next sampling instant, and go to step 3.

For the purpose of comparison, the proposed approach is evaluated with respect to the existing standard MPC approach. However, the model employed and the first module of EKF-based parameter estimation are retained as such in this scheme also. Therefore, the algorithm for adaptive ANN-based MPC for supervisory control consists of steps 1 and 3 of the EKFMPC algorithm, followed by a constrained optimization problem solution based on successive quadratic programming, followed by steps 5 and 6.

EKF has been used for parameter estimation of the ANN model in [19], where the recursive algorithm is shown to perform at least as good as most other second order algorithms with good convergence illustrated through benchmark simulation examples. Huang *et al.* [35] have carried out robust stability analysis of NMPC based on EKF, where it was theoretically shown that the estimated state from EKF exponentially converges to a bounded region even in the presence of plant/model mismatch. They also analyzed the impact of estimation error on the robust stability and offset-free tracking performance of NMPC through simulation studies. Most of the analysis reported in these studies is, in general, applicable to this paper also. Specifically, the stability analysis and offset-free tracking ability of the control strategy proposed in this paper are, respectively, illustrated in Appendixes A and B of Supplementary Information.

III. SEMIBATCH POLYMERIZATION REACTOR

A multiproduct semibatch polymerization reactor industrial case study has been presented by Chylla and Haase [22] as a challenge problem for temperature control. The main hurdles encountered in temperature control in polymerization reactor are variation in physical properties of the material handled within a batch as well as from batch to batch. The details on the recipe considered for simulation in this paper for two products, namely, products A and B, are reported elsewhere [22], [24].

The detailed process model for semibatch polymerization reactor consists of four states (moles of monomer, reactor temperature, outlet jacket temperature, and inlet jacket temperature) and is described by four differential equations and several algebraic equations as follows.

Material balance in terms of moles of monomer is

$$\frac{dn_m}{dt} = F_M - R_P \tag{35}$$

where

$$F_M = \frac{m_M}{\mathrm{MW}_M}, \quad R_p = i(kn_m), \quad k = k_0 \exp\left(\frac{6400}{T+460}\right)\mu^{0.4} \tag{36}$$

where n_m = number of moles of monomer in the reactor (lb · mol), F_M = molar flow rate of monomer into the reactor (lb · mol/min), R_P = rate of polymerization (lb · mol/min), T = reactor temperature (°F), k = first-order kinetic constant (1/min), k_0 = preexponential factor (1/min), μ = product viscosity (cP), and i = impurity factor.

The energy balance around the reactor is given by

$$\begin{aligned}\sum_i m_i C_{pi}\frac{dT}{dt} &= m_M C_{pM}(T_{\mathrm{amb}} - T) + R_p(-\Delta H_P)\\ &\quad - UA(T - T_{\mathrm{jav}}) - (UA)_{\mathrm{loss}}(T - T_{\mathrm{amb}})\end{aligned} \tag{37}$$

where T_{amb} = ambient temperature (°F), U = overall heat transfer coefficient (B.t.u./ft^2 · min ·°F), m_i = mass of component i in the reactor (lb), $i = M$ for monomer, W for water, and S for solids, m_M = mass flow rate of monomer (lb/min), $(UA)_{\mathrm{loss}}$ is heat loss to environment per unit temperature (B.t.u./min ·°F), T_{jav} = average jacket temperature (°F), $-\Delta H_P$is heat of polymerization (B.t.u./lb · mol), A = jacket heat transfer area (ft^2), $c(t)$ = valve opening (0–100%), C_p = specific heat of component i (B.t.u./lb ·°F), and MW_M = molecular weight of the monomer mix (lb/lb · mol).

The exit temperature of the jacket is given by

$$\begin{aligned}m_c C_{\mathrm{pc}}\frac{dT_j^{\mathrm{out}}(t)}{dt} &= \dot{m}_c C_{\mathrm{pc}}\left[T_j^{\mathrm{in}}(t-\theta_1) - T_j^{\mathrm{out}}(t)\right]\\ &\quad + UA(T - T_{\mathrm{jav}})\end{aligned} \tag{38}$$

where

$$T_{\mathrm{jav}} = \frac{T_j^{\mathrm{in}} + T_j^{\mathrm{out}}}{2} \tag{39}$$

where m_c = mass of coolant in jacket (lb), $\dot{m}_c$ = circulation rate (lb/min), C_{pc} = heat capacity of coolant in jacket (B.t.u./lb-°F), θ_1 = transport delay in jacket (min), and θ_2 = transport delay in recirculation loop (min).

The inlet jacket temperature is the delayed exit jacket temperature given by

$$\frac{dT_j^{\mathrm{in}}(t)}{dt} = \frac{dT_j^{\mathrm{out}}(t-\theta_2)}{dt} + \frac{\left(T_j^{\mathrm{out}}(t-\theta_2) - T_j^{\mathrm{in}}(t) + K_p\right)}{\tau_p} \tag{40}$$

where K_p = heating/cooling process gain (°F/%) and τ_p = heating/cooling time constant (min).

The viscosity relation for Product A is given by

$$\mu = 0.032e^{(16.4f)}10^{[2.3(a-1.563)]}. \quad (41)$$

The viscosity relation for Product B is given by

$$\mu = 0.032e^{(119.1f)}10^{[2.3(a-1.563)]} \quad (42)$$

where

$$\begin{aligned} a &= \frac{1000}{T+460};\ f(t) = \frac{s(t)}{bw(t)} \\ h &= 143.4\exp(-5.13 * 10^{-3}\mu_{wall}) \\ \mu_{\text{wall}} &= \mu(T_{\text{wall}});\quad T_{\text{wall}} = \frac{T+T_j}{2} \\ \frac{1}{h_f} &= \{0.000, 0.001, 0.002, 0.003, 0.004\} \\ &\quad \text{for batches } \{1, 2, 3, 4, 5\} \\ s(t) &= s_0 - X(t).tma(t) \\ bw(t) &= s(t) + tma(t)(1 - X(t)) + w_0 \end{aligned} \quad (43)$$

where $s(t)$ and s_0 represent the solids at time t and initial solids, respectively, $bw(t)$ represents the batch weight, $tma(t)$ denotes the total monomer added, $X(t)$ denotes the monomer conversion, and w_0 denotes the initial water content present in the batch, and f denotes the fraction of solids.

The overall heat transfer coefficient is then given by

$$U = 1/\left(\frac{1}{h} + \frac{1}{h_f}\right) \quad (44)$$

where h = film heat transfer coefficient (B.t.u./ft^2·min·°F) and h_f = fouling factor.

The process gain equation is expressed in terms of valve opening as

$$K_p = \left\{\begin{matrix} 0.8 \times (30)^{(-c(t)/50)}\left(T_{\text{inlet}} - T_j^{\text{in}}\right) & 0 \le c(t) < 50 \\ 0 & c(t) = 50 \\ 0.51 \times \left(350 - T_j^{\text{in}}\right)(30)^{(c(t)/50-2)} & 50 < c(t) \le 100 \end{matrix}\right\}. \quad (45)$$

Chylla and Haase [22] have prescribed the acceptable limits for temperature for this system as less than 1°F. The only information available for use in control computation is the specific product, temperature measurement of reaction, jacket inlet water, and jacket exit water, and monomer addition rate. Any controller is expected to perform over five consecutive batches for both products in both the seasons.

IV. Control Configurations for Chylla–Haase Problem

In this paper, the reaction temperature of a multiproduct semibatch polymerization reactor is controlled at its set point using two MPC-based cascade control schemes, i.e., a cascade combination of ANN-EKFMPC with PI (ANN-EKFMPC-PI), i.e., the master controller as ANN-EKFMPC at supervisory level and the slave controller as PI at regulatory level, and ANN-MPC with PI (ANN-MPC-PI) using standard MPC at supervisory level and PI control at regulatory level.

A. ANN-EKFMPC-PI

In this control formulation, a purely data-driven ANN model based on temperature measurements is employed. In this paper, the ANN model, which is used for control computation using EKF formulation, is not an offline trained network. Instead, the parameters of the ANN model (weights) are updated using EKF for parameter estimation and the updated ANN model is then employed for control computation, at every sampling instant.

A single hidden layer ANN model is considered in this paper. The input layer performs the task of scaling the inputs to a range of −5 to 5 and the hidden layer and output layer have sigmoidal activation functions. A fixed configuration of 2-3-1 (input–hidden–output) is considered excluding bias nodes, resulting in a total of 13 weights in the network. The values of output and mean cooling jacket temperature variables at the previous sampling instant, i.e., reactor temperature (T) and T_{jav}, are the inputs to the network and the present reactor temperature are the outputs of the network. The control computations in EKFMPC provide the mean cooling jacket temperature set point $T_{j\text{set}}$ to control the reaction temperature at the desired set point. It is assumed that process gain relation (37) between K_p and $c(t)$ is known. The slave controller is considered as a PI controller to compute K_p, which is converted into the valve opening $c(t)$, and is implemented to track the mean jacket temperature set point $T_{j\text{set}}$. The algorithm listed in Section II for ANN-EKFMPC is employed for implementation of this scheme.

B. ANN-MPC-PI

In this control scheme, the master controller of the previous scheme is replaced with a standard MPC, while retaining the remaining computations including slave control calculations as such. MPC is formulated to control the reaction temperature at the desired set point to compute the mean cooling jacket temperature set point $T_{j\text{set}}$. The algorithm mentioned in Section II for adaptive ANN-MPC is employed for implementation of this scheme.

V. Results and Discussion

A multiproduct semibatch polymerization reactor industrial case study presented by Chylla and Haase [22] is considered for evaluation of the proposed control strategy. The requirements specified include reactor temperature control within ±1 °F throughout each batch where heat transfer characteristics change due to increasing product viscosity, to handle batch to batch variations arising due to changes in fouling factor and seasonal variations in ambient temperature and also to handle variations in the product grade or type.

In this paper, a cascade combination of ANN-EKFMPC-PI and ANN-MPC-PI are used to control the reaction temperature at the desired set point. For the controller, the tuning parameters can be different for each product, but must remain the same from batch to batch for the same product. The tuning of the parameters is based on a reasonable control performance with offset free set point tracking with no/minimum constraint violations over five batches in summer and winter. The performance of the controllers is evaluated by root-mean-square output deviation (RMSOD) values from the set point and the normalized root-mean-square input deviation (NRMSID) values from the nominal input value of 50% (no heating and no cooling) for this system, which are given by

$$\text{RMSOD} = \sqrt{\frac{\sum_{t_{\text{ref}}}^{t_f} (T_{\text{set}} - T)^2}{(t_f - t_{\text{ref}})}} \tag{46}$$

$$\text{NRMSID} = \sqrt{\frac{\sum_{t_{\text{ref}}}^{t_f} (50 - c(t))^2}{(100^2) \times (t_f - t_{\text{ref}})}} \tag{47}$$

where t_{ref} is the time at which the reactor operation switches to phase 2 and t_f is the total batch duration for both the products.

The tuning is carried out for both the products for both the control schemes with reference to the minimization of root-mean-square deviation of the input and the output. For the regulatory level PI controller, the base case tuning is determined using Zeigler and Nichols [36] tuning rules and further fine-tuning is carried out by trial and error to improve the performance. p_0, q, and r relevant to parameter estimation and p_{c0}, q_c, and r_c pertaining to control estimation are considered as the tuning parameters in addition to the prediction horizon N to achieve the best performance with respect to tracking the reaction temperature set point. The final values of the tuned controller parameters for both control schemes are reported in Table I for both the products for both seasons based on RMSOD and NRMSID. The reported parameter values in Table I give the best controller performance for five batches during summer and winter for both the products; however, for summer batches 4 and 5, there is a slight deterioration in control performance for both the products in EKFMPC scheme. Therefore, the parameters are slightly fine-tuned to get better set point tracking for these batches. The fine-tuned parameters for product A are $p_0 = 1 \times 10^{-9}$ and $r = 2 \times 10^{-16}$, and for product B $p_0 = 7 \times 10^{-10}$, $q = 8 \times 10^{-17}$, and $r = 2 \times 10^{-16}$ with the other parameters remaining the same. If p_0 is higher than the tuned value, an offset is observed in the temperature profile; on the other hand, a lower value resulted in a more oscillatory response compared with the tuned value. If r is higher than the tuned value, the predictions are found to be slightly inaccurate, whereas a lower value resulted in a more oscillatory response compared with the tuned value. Lower prediction horizon is found to result in oscillations of increasing magnitude, whereas higher prediction horizon is found to increase the rise time, resulting in large amplitude input oscillations as well as output oscillations. The chosen prediction horizons for summer and winter for both the products are reported in Table I. The move suppression factor is found to influence the oscillatory behavior of the input trajectory. High values lead to increase in overshoot and sluggish responses, whereas low values of move suppression factor result in a highly oscillatory input profile. An appropriate choice is made to balance these two issues and the values are reported in Table I. The three additional

TABLE I

TUNING PARAMETERS FOR ANN-EKFMPC-PI AND ANN-MPC-PI CASCADE CONTROLLERS FOR PRODUCTS A AND B

Control Loop	Parameters	ANN-EKFMPC(m)-PI(s)		ANN-MPC(m)-PI(s)	
		Summer	Winter	Summer	Winter
Product A					
Master controller (m)	p_0	1×10^{-10}	8×10^{-14}	1×10^{-11}	8×10^{-15}
	q	8×10^{-16}	1×10^{-15}	8×10^{-16}	1×10^{-15}
	r	5×10^{-17}	9×10^{-17}	5×10^{-17}	9×10^{-17}
	p_{c0}	3	10	-	-
	q_c	10	10	-	-
	r_c	1	1	-	-
	N_c	1	1	1	1
	N	9	9	11	11
	λ	0.0023	0.0074	0.0035	0.0017
Slave controller (s)	k_{c1}	10	12	10.8	10.8
	k_{c2}	1.9	0.1	2	2
Product B					
Master controller (m)	p_0	9×10^{-11}	1.5×10^{-13}	9×10^{-11}	1.5×10^{-13}
	q	8×10^{-16}	1×10^{-17}	8×10^{-16}	1×10^{-17}
	r	5×10^{-17}	2×10^{-16}	5×10^{-17}	2×10^{-16}
	p_{c0}	3	1	-	-
	q_c	8	8	-	-
	r_c	1	1	-	-
	N_c	1	1	1	1
	N	9	12	9	9
	λ	0.0035	0.0035	0.0017	0.0017
Slave controller (s)	k_{c1}	10	15	10	12
	k_{c2}	2	3	2	1

k_{c1}=Proportional gain for slave control, k_{c2}=Integral gain for slave control.

parameters in EKFMPC (p_{c0}, q_c, r_c) are found to be relatively insensitive with respect to controller performance and nominal values are chosen.

Preliminary results with the ANN-EKFMPC-PI controller incorporating the constraint-handling capability indicated that minor constraint violations during iterative computations lead to large variations in control calculations. Therefore, a correction factor is incorporated into control update equation (21) in order to decrease its contribution to the control calculations. The resulting equation is given as

$$u_k^{++} = u_k^{+} + c_f K c_k^{\text{con}} (\mathbf{y}^{\text{lim}} - \mathbf{y}_c). \tag{48}$$

The correction factor is used as an additional tuning parameter in this control scheme and is chosen as 10^{-5} for both summer and winter for both the products. The same correction factor is used for the terminal constraint control update.

The comparison of the results for both the control schemes for Product A for both the seasons is listed in Table II, whereas the comparison of the results for Product B is reported in Table III. The results indicate that for both the products, the overall average RMSOD and NRMSID values over ten batches (summer and winter) for ANN-EKFMPC-PI are smaller than for ANN-MPC-PI. In general, it is observed that the results for summer batches are better than for winter batches using ANN-EKFMPC-PI, whereas the converse is true with ANN-MPC-PI. It is observed that EKFMPC is able to handle constraints perfectly for all summer batches for both the products, whereas small constraint violations are observed

TABLE II

COMPARISON OF THE PERFORMANCE OF ANN-EKFMPC-PI WITH ANN-MPC-PI FOR CHYLLA–HAASE CHALLENGE CONTROL PROBLEM [22]—PRODUCT A

Product-A Summer Batch No.	**$1/h_f$**	**Root mean square output deviation values (RMSOD)/ Normalized root mean square input deviation values (NRMSID)**			
		ANN-EKFMPC-PI		**ANN-MPC-PI**	
		RMSOD	NRMSID	RMSOD	NRMSID
1	0.000	0.0899	0.0921	0.9618	0.2879
2	0.001	0.0762	0.0858	0.8738	0.2266
3	0.002	0.0806	0.0919	0.8087	0.1898
4	0.003	0.0723	0.0999	0.7953	0.2526
5	0.004	0.0951	0.1205	0.7324	0.2039
Summer Average		***0.0828***	***0.0980***	***0.8344***	***0.2326***
Product-A Winter Batch No.	**$1/h_f$**	**Root mean square output deviation values (RMSOD)/ Normalized root mean square input deviation values (NRMSID)**			
		ANN-EKFMPC-PI		**ANN-MPC-PI**	
		RMSOD	NRMSID	RMSOD	NRMSID
1	0.000	0.2680	0.1806	0.8478	0.2040
2	0.001	0.2655	0.1735	0.8012	0.3158
3	0.002	0.2041	0.1676	0.7229	0.2748
4	0.003	0.3540	0.1701	0.7025	0.2534
5	0.004	0.3247	0.1652	0.6294	0.2211
Winter Average		***0.2834***	***0.1714***	***0.7407***	***0.2538***
Overall Average		***0.1831***	***0.1347***	***0.7875***	***0.2432***

TABLE III

COMPARISON OF THE PERFORMANCE OF ANN-EKFMPC-PI WITH ANN-MPC-PI FOR CHYLLA–HAASE CHALLENGE CONTROL PROBLEM [22]—PRODUCT B

Product-B Summer Batch No.	**$1/h_f$**	**Root mean square output deviation values (RMSOD)/ Normalized root mean square input deviation values (NRMSID)**			
		ANN-EKFMPC-PI		**ANN-MPC-PI**	
		RMSOD	NRMSID	RMSOD	NRMSID
1	0.000	0.1115	0.1084	1.1632	0.3535
2	0.001	0.1093	0.1163	1.1202	0.2290
3	0.002	0.1224	0.1653	1.2614	0.2407
4	0.003	0.1130	0.1438	1.1640	0.3208
5	0.004	0.0985	0.1437	0.7775	0.3145
Summer Average		***0.1109***	***0.1355***	***1.0972***	***0.2917***
Product-B Winter Batch No.	**$1/h_f$**	**Root mean square output deviation values (RMSOD)/ Normalized root mean square input deviation values (NRMSID)**			
		ANN-EKFMPC-PI		**ANN-MPC-PI**	
		RMSOD	NRMSID	RMSOD	NRMSID
1	0.000	0.6081	0.2388	0.7588	0.2849
2	0.001	0.4960	0.2357	0.7402	0.3693
3	0.002	0.4834	0.2390	0.5798	0.3743
4	0.003	0.4898	0.2756	0.4290	0.3874
5	0.004	0.4746	0.2747	0.9979	0.3228
Winter Average		***0.5103***	***0.2527***	***0.7011***	***0.3477***
Overall Average		***0.3106***	***0.1941***	***0.8992***	***0.3197***

in some of the winter batches for short durations, which led to the increase in RMSOD values. Although constraint-handling strategy has been applied, it is observed that the input bounds are already reached due to which the control performance has not improved much. On the other hand, the standard MPC scheme was able to handle constraint violations neither in summer nor in winter in spite of using a constrained optimization solver. Therefore, it is found that in case of summer for both the products, the average RMSOD values of ANN-MPC-PI are about ten times those of ANN-EKFMPC-PI, whereas for winter, this factor varies between 1.5 to 3. The number of input oscillations, as quantified by NRMSID, is also found to be higher with standard MPC compared with EKMPC using a similar move suppression factor.

Figs. 2–5 illustrate the output and input trajectories of master and slave controllers for ANN-EKFMPC-PI and ANN-MPC-PI for products A and B for summer batches 1 and 5. In Figs. 2–5(a)–(c), the output reactor temperature T for both the control schemes, the manipulated input T_{jset} and mean jacket T_{jav} temperature profiles for the cascade master EKFMPC and standard MPC controllers, and the corresponding valve opening $c(t)$ values are represented, respectively. ANN parameters for standard MPC and EKFMPC are represented in Figs. 2–5(d) and (e), respectively.

Figs. 2–5 clearly illustrate that throughout the batch duration, there are no constraint violations (requirement being

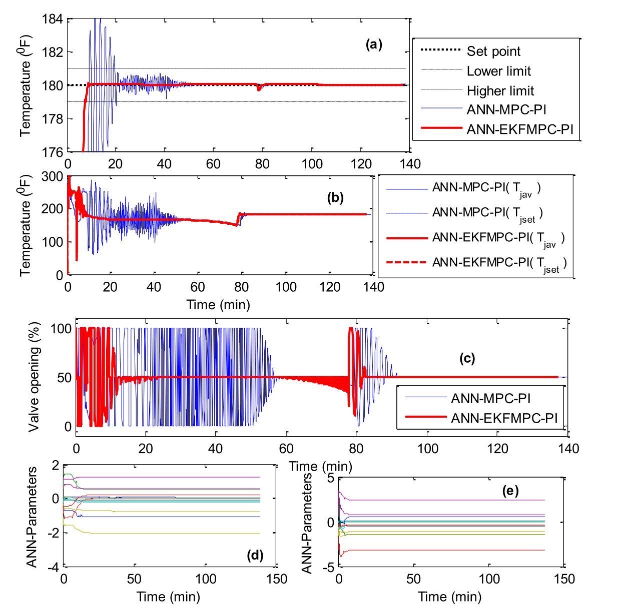

Fig. 2. Comparison of the performances of ANN-MPC-PI and ANN-EKFMPC-PI cascade controllers—Product A for summer batch 1. (a) Reactor temperature profiles. (b) Mean jacket temperature profiles. (c) Input profiles. (d) ANN parameters (ANN-MPC-PI). (e) ANN parameters (ANN-EKFMPC-PI).

maintenance within ±1 °F) with ANN-EKFMPC-PI, whereas with ANN-MPC control, reactor temperature is found to exhibit constraint violations and the corresponding input

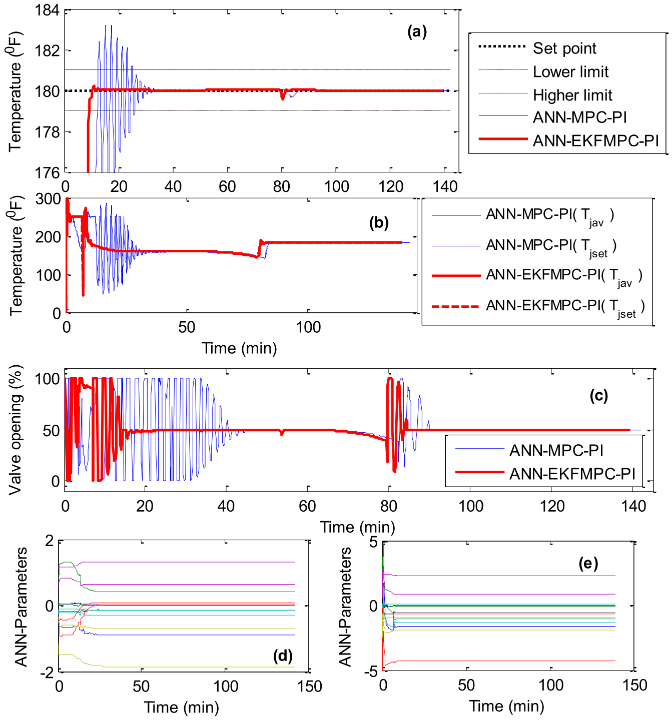

Fig. 3. Comparison of the performances of ANN-MPC-PI and ANN-EKFMPC-PI cascade controllers—Product A for summer batch 5. (a) Reactor temperature profiles. (b) Mean jacket temperature profiles. (c) Input profiles. (d) ANN parameters (ANN-MPC-PI). (e) ANN parameters (ANN-EKFMPC-PI).

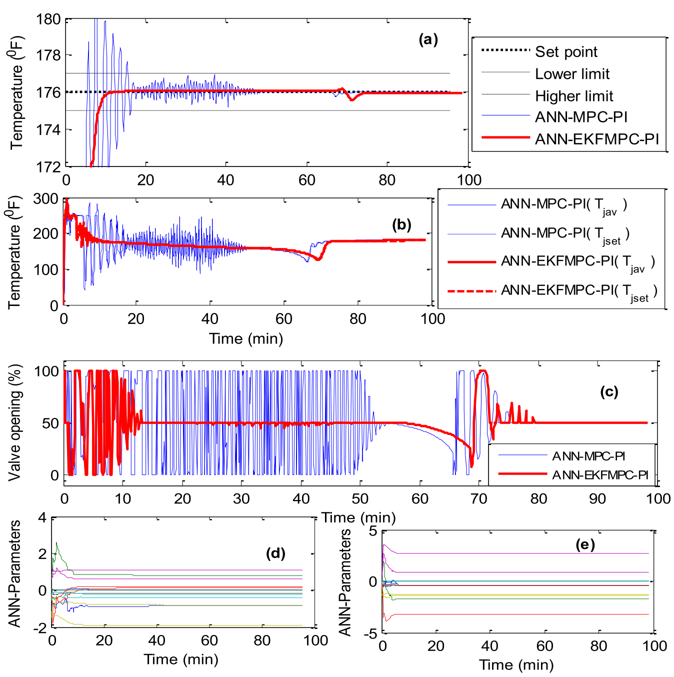

Fig. 4. Comparison of the performances of ANN-MPC-PI and ANN-EKFMPC-PI cascade controllers—Product B for summer batch 1. (a) Reactor temperature profiles. (b) Mean jacket temperature profiles. (c) Input profiles. (d) ANN parameters (ANN-MPC-PI). (e) ANN parameters (ANN-EKFMPC-PI).

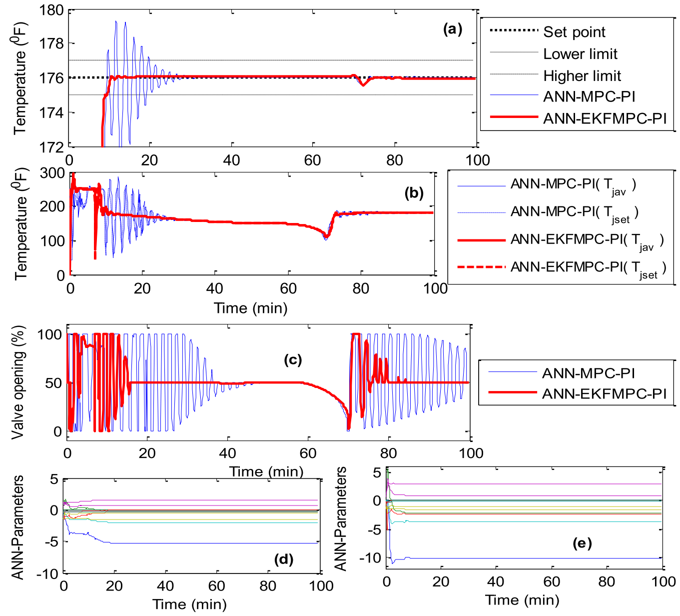

Fig. 5. Comparison of the performances of ANN-MPC-PI and ANN-EKFMPC-PI cascade controllers—Product B for summer batch 5. (a) Reactor temperature profiles. (b) Mean jacket temperature profiles. (c) Input profiles. (d) ANN parameters (ANN-MPC-PI). (e) ANN parameters (ANN-EKFMPC-PI).

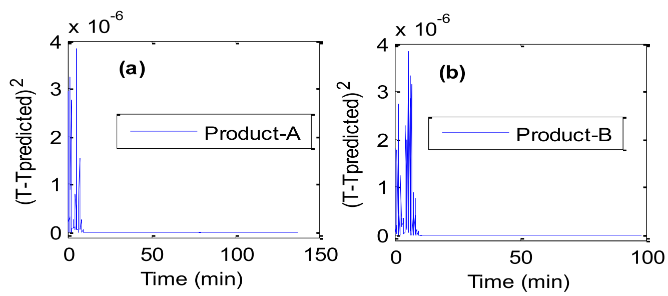

Fig. 6. Process model mismatch profiles for ANN-EKFMPC-PI cascade control. (a) Product A summer batch 1. (b) Product B summer batch 1.

profiles have oscillations of very large amplitude. The results clearly illustrate that EKFMPC gives tighter temperature control compared with the standard MPC scheme. The possible reason for better performance of ANN-EKFMPC-PI is its additional flexibility (in terms of three additional EKF controller tuning parameters). To further illustrate the convergence of EKF parameter estimation for the ANN model, the process/model mismatch profiles (squared deviation between instantaneous values of prediction and measurement) for both the products are plotted in Fig. 6, which clearly indicate the fast convergence leading to robust performance of the ANN-EKFMPC controller.

In addition to the variations in heat transfer coefficients expressed as batch-to-batch variations in the above discussion for both the products in both the seasons, the performance of the proposed controller, namely, ANN-EKFMPC-PI cascade controller, is also evaluated in the presence of a few other disturbances for the first batch of summer for both the products. The unmeasured disturbances considered are load disturbance in monomer feed flow rate, impurity factor in the rate expression of different magnitudes in both the directions (+/−), and mismatches in transportation delays of jacket and recirculation loop. Table IV illustrates the control performance in the presence of disturbances in monomer

TABLE IV

EFFECT OF OTHER DISTURBANCES ON CONTROL PERFORMANCE USING ANN-EKFMPC-PI—PRODUCTS A AND B (SUMMER BATCH1)

EFFECT OF UNMEASURED DISTURBANCES					
		Product A		Product B	
Disturbances	**Variations**	**RMSOD**	**NRMSID**	**RMSOD**	**NRMSID**
base case	i=1; no load disturbance; θ_{1d}=3;θ_{2d}=2	0.0899	0.0921	0.1115	0.1076
impurity factor in rate expression	i=0.9 (-10%)	0.0901	0.0914	0.1082	0.1057
	i=1.1(+10%)	0.0902	0.0924	0.1145	0.1090
load disturbance in monomer feed flow rate	-10% flow disturbance	0.0877	0.0893	0.1066	0.1020
	+10% flow disturbance	0.0920	0.0953	0.1179	0.1146
transportation delays in recirculation loop	θ_{1d}=4;θ_{2d} = 2	0.0755	0.1797	0.1072	0.1477
	θ_{1d}=3;θ_{2d} = 3	0.0792	0.0908	0.1058	0.1146
	θ_{1d}=3;θ_{2d} =1	0.0719	0.1056	0.1204	0.1243

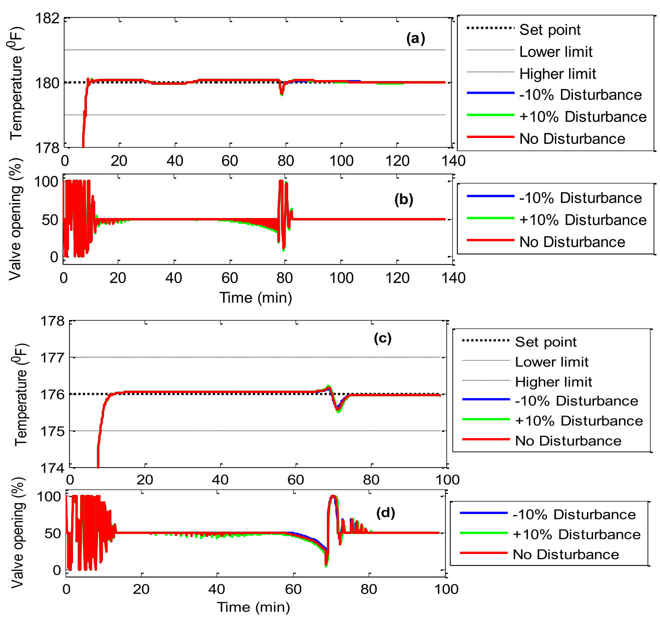

Fig. 7. ANN-EKFMPC-PI cascade controller performance with disturbance rejection of unmeasured monomer feed disturbance for summer batch 1. (a) Master control output profiles for Product A. (b) Slave controller input profile for Product A. (c) Master control output profiles for Product B. (d) Slave controller input profile for Product B.

feed flow rate, impurity factor, and transport delay, where the RMSOD and NRMSID for the cases with disturbances are compared with those for the base case, while using the same controller tuning parameters. The ability of the proposed control strategy to handle all these disturbances is clearly illustrated from Table IV efficiently.

The effect of disturbance rejection is also illustrated in Figs. 7 and 8, where the output and input trajectories for the ANN-EKFMPC-PI controller for Products A and B are plotted. The master controller output profile and the slave controller input profile are illustrated in Figs. 7 and 8(a) and (b),

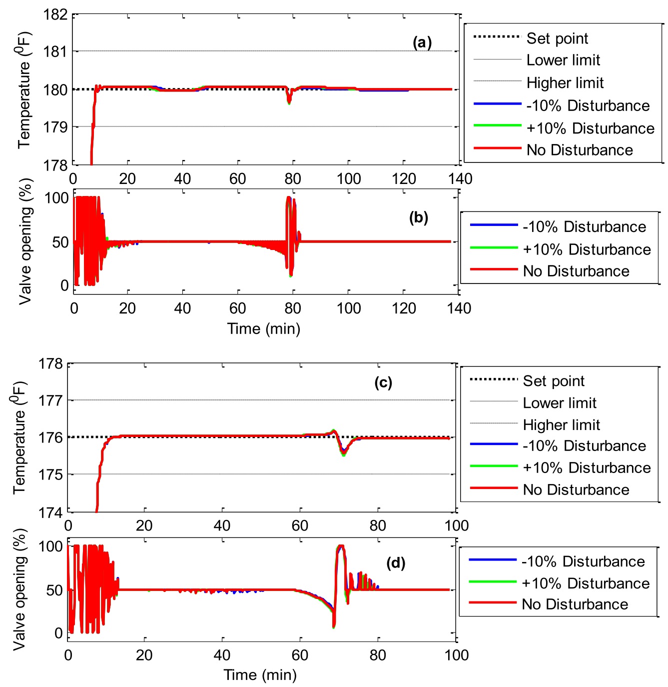

Fig. 8. ANN-EKFMPC-PI cascade controller performance with disturbance rejection of unmeasured impurity factor for summer batch 1. (a) Master control output profiles for Product A. (b) Slave controller input profile for Product A. (c) Master control output profiles for Product B. (d) Slave controller input profile for Product B.

respectively, for product A, and in Figs. 7 and 8(c) and (d), respectively, for product B.

Figs. 7 and 8 illustrate that there is no visible difference in the response with the variation of unmeasured disturbance in monomer feed flow rate and impurity factor in the rate expression for products A and B by ANN-EKFMPC-PI. This indicates that the proposed ANN-EKFMPC-PI controller is robust enough to handle unmeasured disturbances. Further, the process model mismatch during the entire batch is also illustrated in Fig. 6, which clearly shows that the mismatch even at the initial stage is of the order of 10^{-6} and it approaches zero very quickly.

In general, stability of a controller is assessed by defining a Lyapunov function. As reported in Appendix A of Supplementary Information, the objective function for MPC is considered as a Lyapunov function. In order to illustrate the stability of the simulation system reported, this objective function is plotted as a function of time in Figs. 9(a) and 10(a) for products A and B, respectively. Figs. 9(a) and 10(a) clearly show that the proposed controller exhibits the property of stability, although over a short initial period the function is not strictly decreasing possibly due to the minor process/model mismatch during this period (as shown in Fig. 6).

The offset-free tracking property of the proposed controller is illustrated in Appendix B of Supplementary Information. Further, for this system, the actual error, namely, the squared difference between the set point and the process measurement, is computed throughout the batch duration and is plotted in Figs. 9(b) and (c) and 10(b) and (c) for products A and B, respectively. The error in the two phases (reagent addition with temperature control and no reagent addition with temperature

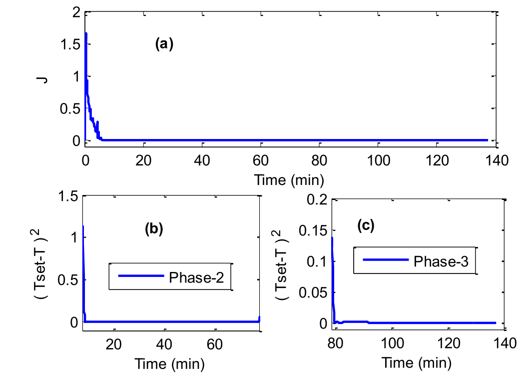

Fig. 9. Profiles representing (a) stability and (b) and (c) offset-free performance for Product-A, where $J = \sum_{i=1}^{N} (T_{\text{set}} - \hat{\tilde{T}}_i)^2 + \lambda \sum_{j=1}^{N_c} (T_{\text{jset},j} - T_{\text{jset},j}^{\text{old}})^2$.

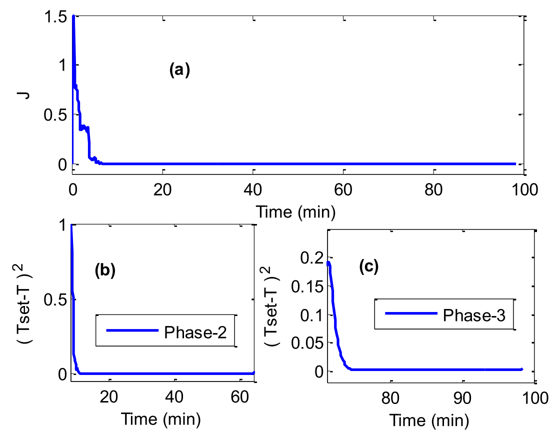

Fig. 10. Profiles representing (a) stability and (b) and (c) offset-free performance for Product-B, where $J = \sum_{i=1}^{N} (T_{\text{set}} - \hat{\tilde{T}}_i)^2 + \lambda \sum_{j=1}^{N_c} (T_{\text{jset},j} - T_{\text{jset},j}^{\text{old}})^2$.

control) are plotted separately since they represent different operating regions. Figs. 9(b) and (c) and 10(b) and (c) clearly illustrate the offset-free tracking performance of the proposed controller.

An analysis of the results obtained for the multiproduct semibatch polymerization reactor control problem shows that the cascade control scheme ANN-EKFMPC-PI has exhibited better performance than the ANN-MPC-PI control scheme for all the cases explored. The proposed approach is found be versatile and has yielded performance comparable to most of the first-principles-model-based control formulations for this system although the only information employed is the temperature measurements.

VI. Conclusion

In this paper, a novel MPC formulation based on EKF employing an adaptive ANN model is proposed for supervisory control and is illustrated for set point tracking of reactor temperature of an industrial multiproduct semibatch polymerization reactor challenge problem. The proposed approach is formulated incorporating all aspects of MPC including move suppression factor for control effort minimization and constraint-handling capability. The performance of the proposed control approach is compared with a standard MPC algorithm using the same ANN model with EKF for parameter estimation online. In both the approaches, the regulatory control loop is a PI controller to track the average jacket temperature set point. The proposed control scheme is used to control the reaction temperature in the presence of disturbances, i.e., seasonal variations and change in heat transfer characteristics during the run as well as from batch to batch. ANN-EKFMPC-PI is found to give better performance over standard MPC approach in terms of output tracking as well as minimum input oscillations, as illustrated by the RMSOD and NRMSID values over ten batches (in both seasons with different fouling factors) for two products A and B. Further, the proposed approach is able to exhibit performance with no constraint violations in summer and minimum constraint violations in winter with relatively smooth input profiles, whereas the standard MPC-based approach was found to be incapable of handling constraints in all the batches and the input profiles were also found to be highly oscillatory. The effect of other disturbances, such as variations in impurity factor, feed flow rate, and mismatches in transportation delays of jacket and recirculation loop, on control performance is evaluated for the both the products with ANN-EKFMPC-PI, and the results indicate a reasonably good control performance and that the variation in the reactor temperature error over the entire batch duration is minimum. For Product A, the variation of the reactor temperature error with time is in the range of 0.1 °F in the positive direction and 0.38 °F in the negative direction (+0.06 and −0.21 K), whereas for Product B, it is in the range of 0.16 °F in the positive direction and 0.42 °F in the negative direction (+0.09 and −0.23 K), from the set point, falling well within the range of ±1 °F (±0.6 K) for a problem that has been benchmarked as a challenge problem for control. The proposed approach is found be versatile although very limited information is employed.

References

[1] L. T. Biegler and J. B. Rawlings, "Optimization approaches to nonlinear model predictive control," in *Proc. 4th Int. Conf. Chem. Process Control*, 1993, pp. 543–571.

[2] M. A. Henson, "Nonlinear model predictive control: Current status and future directions," *Comput. Chem. Eng.*, vol. 23, no. 2, pp. 187–202, 1998.

[3] M. Morari and J. H. Lee, "Model predictive control: Past, present and future," *Comput. Chem. Eng.*, vol. 23, nos. 4–5, pp. 667–682, May 1999.

[4] V. Mahindrakar and J. Hahn, "Model predictive control of reactive distillation for benzene hydrogenation," *Control Eng. Pract.*, vol. 52, pp. 103–113, Jul. 2016.

[5] V. Ghaffari, S. V. Naghavi, and A. A. Safavi, "Robust model predictive control of a class of uncertain nonlinear systems with application to typical CSTR problems," *J. Process Control*, vol. 23, no. 4, pp. 493–499, 2013.

[6] T. Peterson, E. Hernández, Y. Arkun, and F. J. Schork, "A nonlinear DMC algorithm and its application to a semibatch polymerization reactor," *Chem. Eng. Sci.*, vol. 47, no. 4, pp. 737–753, 1992.

[7] A. Karaduman, H. Oguz, and R. Berber, "Nonlinear model predictive control of a batch polymerization reactor," *IChemE-Adv. Process Control*, vol. 4, pp. 203–210, 1995.

[8] Z. K. Nagy and R. D. Braatz, "Robust nonlinear model predictive control of batch processes," *AIChE J.*, vol. 49, no. 7, pp. 1776–1786, 2003.

[9] S. Tebbani, D. Dumur, G. Hafidi, and A. V. Wouwer, "Nonlinear predictive control of fed-batch cultures of escherichia coli," *Chem. Eng. Technol.*, vol. 33, no. 7, pp. 1112–1124, 2010.

[10] S. Lucia, T. Finkler, and S. Engell, "Multi-stage nonlinear model predictive control applied to a semi-batch polymerization reactor under uncertainty," *J. Process Control*, vol. 23, no. 9, pp. 1306–1319, 2013.
[11] K. Y. Rani and S. C. Patwardhan, "Data-driven modeling and optimization of semibatch reactors using artificial neural networks," *Ind. Eng. Chem. Res.*, vol. 43, no. 23, pp. 7539–7551, 2004.
[12] J. Chen and T.-C. Huang, "Applying neural networks to on-line updated PID controllers for nonlinear process control," *J. Process Control*, vol. 14, no. 2, pp. 211–230, 2004.
[13] Z. Xiong and J. Zhang, "A batch-to-batch iterative optimal control strategy based on recurrent neural network models," *J. Process Control*, vol. 15, no. 1, pp. 11–21, 2005.
[14] A. S. Kumar and Z. Ahmad, "Neural network model predictive control of non-linear biopolymerization process," in *Proc. 6th Int. Conf. Process Syst. Eng. (PSE ASIA)*, Jun. 2013, pp. 25–27.
[15] P. D. Vallie're and D. Bonvin, "Application of estimation techniques to batch reactors—II. Experimental studies in state and parameter estimation," *Comput. Chem. Eng.*, vol. 13, nos. 1–2, pp. 11–20, 1989.
[16] D. J. Kozub and J. F. MacGregor, "State estimation for semi-batch polymerization reactors," *Chem. Eng. Sci.*, vol. 47, no. 5, pp. 1047–1062, 1992.
[17] M. A. Myers and R. H. Luecke, "Process control applications of an extended Kalman filter algorithm," *Comput. Chem. Eng.*, vol. 15, no. 12, pp. 853–857, 1991.
[18] F. Gao, F. Wang, and M. Li, "A neural-network-based nonlinear controller using an extended kalman filter," *Ind. Eng. Chem. Res.*, vol. 38, no. 6, pp. 2345–2349, 1999.
[19] I. Rivals and L. Personnaz, "A recursive algorithm based on the extended Kalman filter for the training of feedforward neural models," *Neurocomputing*, vol. 20, nos. 1–3, pp. 279–294, 1998.
[20] K. Y. Rani and M. Swetha, "Extended kalman filter controller: First principles models to neural networks," *Chem. Eng. Commun.*, vol. 193, no. 10, pp. 1294–1320, 2006.
[21] A. Saengchan, P. Kittisupakorn, W. Paengjuntuek, and A. Arpornwichanop, "Improvement of batch crystallization control under uncertain kinetic parameters by model predictive control," *J. Ind. Eng. Chem.*, vol. 17, no. 3, pp. 430–438, 2011.
[22] R. W. Chylla and D. R. Haase, "Temperature control of semi-batch polymerization reactors," *Comput. Chem. Eng.*, vol. 17, no. 3, pp. 257–264, 1993.
[23] K. Y. Rani, "Sensitivity compensating nonlinear control: Exact model based approach," *J. Process Control*, vol. 22, no. 3, pp. 564–582, 2012.
[24] R. Kamesh, P. S. Reddy, and K. Y. Rani, "Comparative study of different cascade control configurations for a multiproduct semi-batch polymerization reactor," *Ind. Eng. Chem. Res*, vol. 53, no. 38, pp. 14735–14754, 2014.
[25] T. Clarke-Pringle and J. F. MacGregor, "Nonlinear adaptive temperature control of multi-product, semi-batch polymerization reactors," *Comput. Chem. Eng.*, vol. 21, no. 12, pp. 1395–1409, 1997.
[26] K. Graichen, V. Hagenmeyer, and M. Zeitz, "Feedforward control with online parameter estimation applied to the Chylla—Haase reactor benchmark," *J. Process Control*, vol. 16, no. 7, pp. 733–745, 2006.
[27] D. Vasanthi, B. Pranavamoorthy, and N. Pappa, "Design of a self-tuning regulator for temperature control of a polymerization reactor," *ISA Trans.*, vol. 51, no. 1, pp. 22–29, 2012.
[28] A. Helbig, O. Abel, A. M'hamdi, and W. Marquardt, "Analysis and nonlinear model predictive control of the Chylla—Haase benchmark problem," in *Proc. Int. Conf. Control UKACC*, 1996, pp. 1171–1177.
[29] C. W. Ng and M. A. Hussain, "Hybrid neural network—Prior knowledge model in temperature control of a semi-batch polymerization process," *Chem. Eng. Process., Process Intensification*, vol. 43, no. 4, pp. 559–570, 2004.
[30] K. Y. Rani, "Sensitivity compensating control: Data-driven model based adaptive approach," *J. Process Control*, vol. 21, no. 9, pp. 1265–1286, 2011.
[31] K. Y. Rani and S. C. Patwardhan, "Data-driven Model based control of a multi-product semi-batch polymerization reactor," *Chem. Eng. Res. Design*, vol. 85, no. 10, pp. 1397–1406, 2007.
[32] B. Ganesh, V. V. Kumar, and K. Y. Rani, "Modeling of batch processes using explicitly time-dependent artificial neural networks," *IEEE Trans. Neural Netw. Learn. Syst.*, vol. 25, no. 5, pp. 970–979, May 2014.
[33] S. Krämer and R. Gesthuisen, "Simultaneous estimation of the heat of reaction and the heat transfer coefficient by calorimetry: Estimation problems due to model simplification and high jacket flow rates—Theoretical development," *Chem. Eng. Sci.*, vol. 60, no. 15, pp. 4233–4248, 2005.
[34] S. Ungarala, E. Dolence, and K. Li, "Constrained extended Kalman filter for nonlinear state estimation," in *Proc. 8th IFAC Symp. Dynamic Control Process Syst.*, Cancún, Mexico, 2007, pp. 63–68.
[35] R. Huang, S. C. Patwardhan, and L. T. Biegler, "Robust stability of nonlinear model predictive control based on extended Kalman filter," *J. Process Control*, vol. 22, no. 1, pp. 82–89, 2012.
[36] J. G. Ziegler and N. B. Nichols, "Optimum settings for automatic controllers," *ASME Trans.*, vol. 64, no. 11, pp. 759–765, 1942.

Reddi Kamesh received the B.Tech. degree in chemical engineering from Acharya Nagarjuna University, Guntur, India, in 2011, and the M.Tech. degree in process engineering science from the CSIR-Indian Institute of Chemical Technology (IICT), Academy of Scientific and Innovative Research, Hyderabad, India, in 2014, where he is currently pursuing the Ph.D. degree.

From 2012 to 2016, he was a Trainee Scientist with the Chemical Engineering Division, CSIR-IICT, where he is currently a Scientist. He has authored one book chapter, and over 26 papers in peer-reviewed international and national journals and proceedings of international and national conferences. His current research interests include dynamic modeling, optimization, and novel model predictive control strategies based on extended Kalman filter, fuzzy/neural modeling and control, data-driven modeling, process development, design and intensification, and advanced control of chemical and biochemical engineering systems.

Mr. Kamesh was a recipient of the Ambuja Young Researchers Award in 2014 from the Indian Institute of Chemical Engineers, the Best Poster Presentation Award at the Indo-US Conference on Advanced Lignocellulosic Biofuels in 2014, CSIR-IICT, Hyderabad, and the Best Poster Presentation Award at Indus Cop, Workshop on Intensification and Up-scaling of Continuous Processes in 2013, CSIR-National Chemical Laboratory, Pune, India.

Kalipatnapu Yamuna Rani received the B.Tech. degree in chemical engineering from Osmania University, Hyderabad, India, in 1986, and the M.Tech. and Ph.D. degrees in chemical engineering from IIT Madras, Madras, India, in 1988 and 2002, respectively.

She has been with the Chemical Engineering Division at the Indian Institute of Chemical Technology, Hyderabad, since 1990, in various scientific positions, and is currently a Senior Principal Scientist. She is also a Professor with the Academy of Scientific and Innovative Research, Hyderabad, in the discipline of Engineering Sciences. She has authored two books, two book chapters, and about 150 papers in peer-reviewed international and national journals and proceedings of international and national conferences. Her current research interests include dynamic modeling, optimization, product modeling and design, data-driven modeling, and advanced control of chemical and biochemical engineering systems.

Dr. Rani was a recipient of the Dr. Subba Raju Memorial Prize and medal from IIT, Madras, the Kuloor Memorial Award for the Best Technical Paper published in Indian Chemical Engineer Transactions, the DAAD (German Academic Exchange Service) Fellowship for 16 months in Germany, and the CSIR Young Scientist Award for basic research in Engineering Sciences. She has been a Reviewer for Chemical Engineering journals of repute.